Z. Kristallogr. Suppl. **26** (2007) 139-145

In-situ powder diffraction in high magnetic fields

V.K. Pecharsky[1,2,*], Ya. Mudryk[1], K.A. Gschneidner, Jr.[1,2]

[1]Ames Laboratory, Iowa State University, Ames, Iowa 50011-3020, USA
[2]Department of Materials Science and Engineering, Iowa State University, Ames, IA 50011-2300, USA
[*] Contact author; e-mail: vitkp@ameslab.gov

Keywords: powder diffraction, phase transformations, temperature, magnetic field.

Abstract. By coupling a rotating anode powder diffractometer with a continuous-flow liquid helium-cooled cryostat and a split-coil superconducting magnet, Rietveld-quality powder diffraction data have been obtained between 5 and 315 K in magnetic fields reaching 4 T. A typical experiment quantifying both the phase composition and changes in the unit cell dimensions and phase volume(s) may be carried out in as little as ten to twenty minutes. A few hours long experiment is sufficient to provide detailed information about the individual atomic parameters. Both massive and subtle field-induced structural changes have been detected, providing structural data needed to develop a better understanding of structure-property relationships of solids.

Introduction

Temperature and pressure induced polymorphism is common compared to structural rearrangements triggered by magnetic field. While the former are routinely probed by temperature- and/or pressure-dependent powder diffraction [1,2], the most common tools employed in detecting magnetic field induced structural changes are field-dependent measurements of bulk physical properties, such as the electrical resistance, magnetization, and strain. Discontinuities in the behavior of these macroscopic properties are usually taken as evidence of the underlying structural changes, but they do not provide any clues about the atomic-scale mechanism(s).

Modern x-ray powder diffraction method is a powerful tool for characterization of crystalline solids. Whether used for phase identification or for detailed atomic-scale structural analysis, it provides highly accurate information in a quick and simple fashion [3-5]. Neutron powder diffraction is occasionally employed to study magnetic field induced effects [6-8], but relatively low resolution of the data makes it difficult to extract reliable crystallographic information, especially for complex structures [9]. The use of low energy thermal neutrons improves the resolution but limits the volume of reciprocal space that can be examined experimentally. Furthermore, high absorption cross section of the naturally occurring mixtures of isotopes of certain chemical elements (one well-known example is Gd) often makes it diffi-

cult or even impossible to carry out magnetic field dependent neutron powder diffraction experiments.

In the past, x-ray powder diffraction in applied magnetic fields has been employed in a limited capacity to study structural changes. However, due to severe geometrical constraints, only a single Bragg peak or a small and/or poorly resolved range of reciprocal space can be examined and the atomic scale structural information was impossible to extract from the collected diffraction data [10-13]. Only recently, laboratory instruments capable of collecting x-ray powder diffraction data below room temperature in magnetic fields reaching 7 T have been built and tested [14-16]. Performance of one of these instruments, originally described in [15,16], is briefly reviewed here.

The instrument

The instrument (figure 1) consists of three components: a diffractometer, a split coil superconducting magnet, and a continuous-flow cryostat. The diffractometer is a standard Rigaku TTRAX system equipped with a wide-angle theta/theta goniometer and an 18 kW rotating anode x-ray source. The instrument employs Mo Kα radiation in the Bragg-Brentano geometry. A combination of a diffracted beam monochromator and a scintillation detector provides excellent resolution and a high signal to noise ratio of the data.

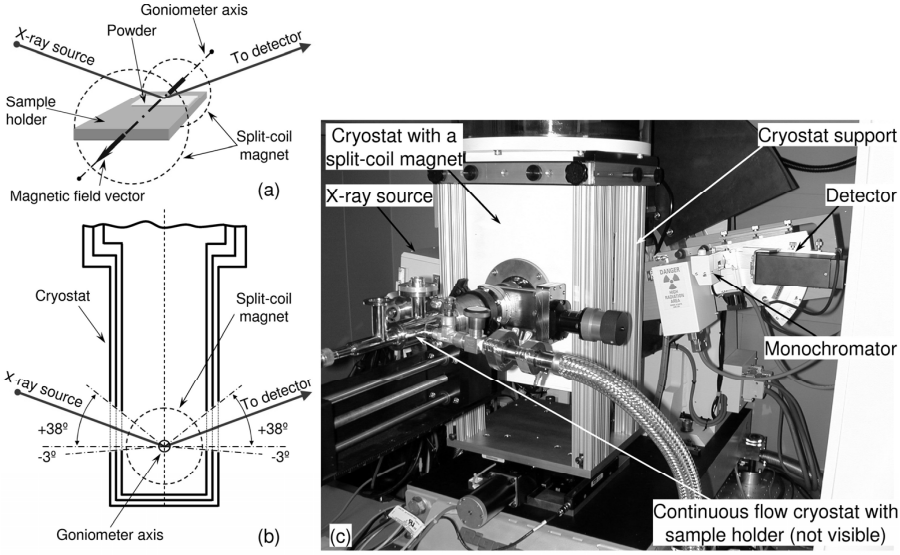

Figure 1. The schematic of a sample holder surrounded by a split coil magnet (a); the schematic of a cryostat holding the split coil magnet (b); tail of the cryostat mounted on the goniometer (c).

Figure 1c illustrates the bottom of a custom designed optical-access split-coil superconducting magnet cryostat (Janis Research) positioned between the detector and x-ray source arms of the diffractometer. This arrangement allows the sample (figure 1a) to be positioned simi-

lar to the standard Rigaku sample holders while being maintained between the magnet coils. The magnetic field vector is coplanar to the surface of the sample and collinear to the goniometer axis. The split-coil magnet (figure 1b, c) provides a uniform magnetic field from 0 to 4 T around the sample. The field is homogeneous to within 1% in 1 cm^3 volume. The optical windows (figure 1b) allow a continuous sampling range of -6 to 76º in 2θ, which enables measurements of reciprocal lattice vectors that are at or less than 1.77 $Å^{-1}$ ($d > 0.564$ Å) when employing Mo Kα radiation ($\lambda \cong 0.71$ Å).

Field-dependent structural changes in Gd_5Ge_4

Over the past ten years, the R_5T_4 compounds (R = rare earth metal, T = Si and Ge) have been extensively studied because many members of the family exhibit interesting interplay between crystallography and magnetism [17]. According to bulk magnetisation data [18-20], the ground state of Gd_5Ge_4 is an antiferromagnet (AFM). When Gd_5Ge_4 is exposed to a magnetic field exceeding ~1 T, a ferromagnetic (FM) state is induced irreversibly below ~10 K, partly reversibly between 10 and 20 K and fully reversibly above ~20 K. The changeover from the irreversible to reversible behavior is related to the existence of a frozen, glass-like state [21], which is reflected in the low temperature part of the *B-T* phase diagram of the compound shown in figure 2a. We note that this frozen state retains long range crystallographic and magnetic order.

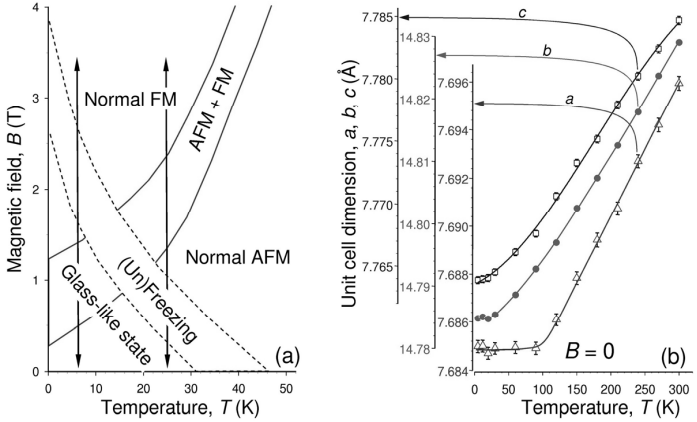

Figure 2. The magnetic phase diagram of Gd_5Ge_4 below 50 K (a) and temperature dependencies of the unit cell dimensions of Gd_5Ge_4 in a zero magnetic field (b). The arrows in (a) correspond to the isothermal field cycles illustrated in figures 3 and 4.

In-situ x-ray powder diffraction data prove that magnetism of Gd_5Ge_4 is closely related to its crystallography. Thus, as long as the compound remains AFM, it maintains the Sm_5Ge_4-type structure and the lattice parameters of the material are anisotropically reduced upon cooling from 300 to 5 K in a zero magnetic field (figure 2b). Isothermal exposure to an increasing magnetic field at 6.1 K results in a structural transition that begins around 1.5 T and is nearly complete at 2 T; this field induced transformation is irreversible (figure 3a and 3b). The

dependence of the crystal structure of Gd_5Ge_4 on the magnetic field is different when the magnetic field is cycled isothermally at 25 K. Similar to the behaviour at 6.1 K, the low magnetic field crystal structure transforms into the high magnetic field allotrope between 1.5 and 2 T, but when the magnetic field is reduced, the zero magnetic field diffraction patterns are restored between 1.5 and 1 T (figure 4a and 4b) displaying a ~1 T hysteresis.

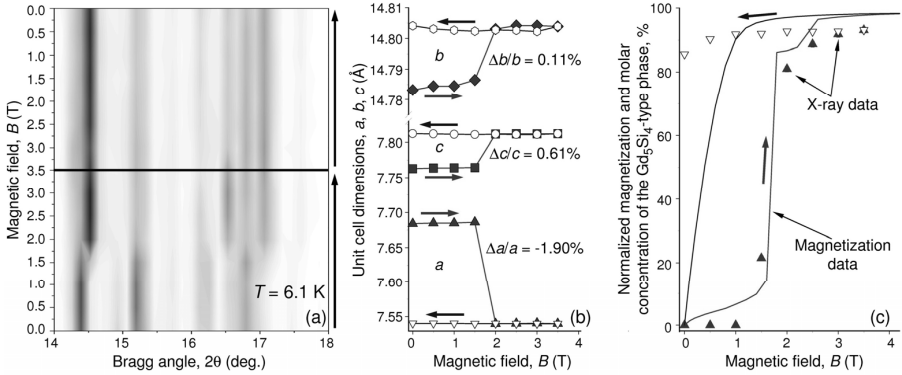

Figure 3. Fragments of the powder diffraction patterns of Gd_5Ge_4 collected at 6.1 K with the magnetic field cycled from 0 to 3.5 T and back to 0 as shown by vertical arrows (a); unit cell dimensions of the majority phase (b), and normalized magnetization and fraction (in %) of the Gd_5Si_4–type structure (c) as functions of magnetic field. In (a), the darker the color, the higher the intensity.

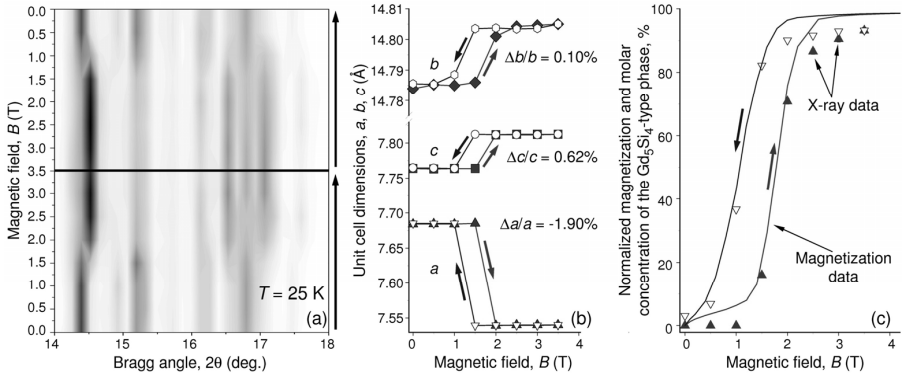

Figure 4. Fragments of the powder diffraction patterns of Gd_5Ge_4 collected at 25 K with the magnetic field cycled from 0 to 3.5 T and back to 0 as shown by vertical arrows (a); unit cell dimensions of the majority phase (b), and normalized magnetization and fraction (in %) of the Gd_5Si_4–type structure (c) as functions of magnetic field. In (a), the darker the color, the higher the intensity.

The irreversibility and reversibility of the magnetic field induced structural transition in Gd_5Ge_4 closely follows the behavior of the magnetization (and the underlying magnetic structure of the compound). The amount of the Gd_5Si_4–type structure formed at 6.1 K by an increasing magnetic field follows the initial magnetization path, figure 3c. Upon removal of the field, Gd_5Ge_4 remains ferromagnetic. Consistent with macroscopic magnetism, the sys-

tem preserves the high magnetic field Gd_5Si_4–type structure, which is ferromagnetic, and whose concentration is only slightly reduced from ~93 to ~86 % when the magnetic field is lowered isothermally to 0. At 25 K, where the FM – AFM transformation is reversible, both the initial magnetization and the subsequent demagnetization paths are followed with high precision by the concentration of the Gd_5Si_4–type structure, see figure 4c.

As follows from Rietveld refinement [15,22], the low magnetic field crystal structures of Gd_5Ge_4 observed at 6.1 K and 25 K are identical to one another, and so are the high magnetic field allotropes. The former belongs to the Sm_5Ge_4-type [23] and the latter to the Gd_5Si_4-type structure [24]. Hence, the glass-like region (figure 2a) is the result of low thermal energy as T approaches 0, which becomes insufficient to overcome the difference in strain energies between the high- and low-magnetic field allotropes of Gd_5Ge_4.

Magnetic field and the nature of phase transition in $DyCo_2$

The series of RCo_2 Laves phase compounds has been broadly studied because several of its members (i.e., those with R = Dy, Ho, and Er) exhibit first order magnetic phase transitions and itinerant electron metamagnetism [25], while other compounds formed by heavy lanthanides (Gd, Tb and Tm) order magnetically *via* second order phase transformations. Furthermore, the application of a magnetic field causes a gradual increase of T_C and a change of the first order phase transition towards a second order phase transformation in some RCo_2 compounds [26].

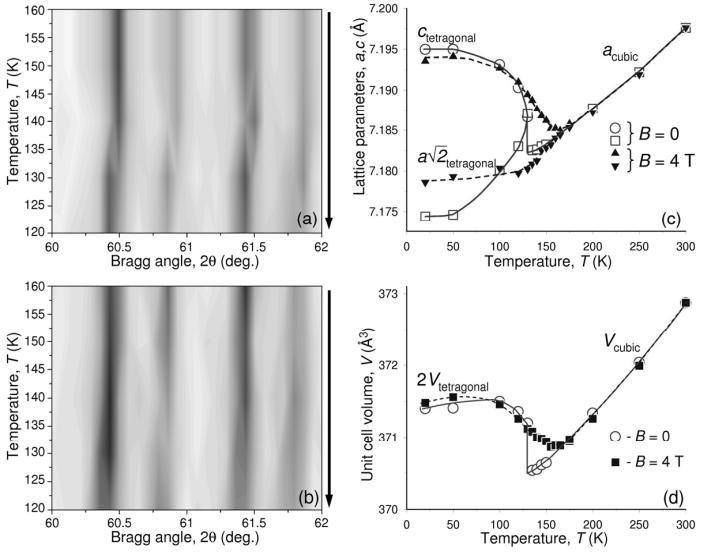

Figure 5. Fragments of the powder diffraction patterns of$DyCo_2$ collected in 0 (a) and 4 T (b) magnetic fields, and behavior of the lattice parameters (c) and unit cell volume (d) as functions of temperature. In (c), open circles and open squares represent zero field data, and solid up- and down- triangles represent 4 T data. In (d), open circles represent zero field data, and solid squares represent 4 T data.

Figure 5 shows results of temperature- and magnetic field-dependent x-ray powder diffraction study of $DyCo_2$. When cooled in a zero magnetic field, the system undergoes a cubic-to-tetragonal distortion (figure 5a, 5c). At the Curie temperature (between 130 and 140 K), the phase volume changes discontinuously by about 0.2% (figure 5d), which is also clearly seen from the discontinuous displacements of the Bragg peaks in figure 5a. This behavior is consistent with the first order nature of the ferrimagnetic ordering in $DyCo_2$. When the compound is cooled in a 4 T magnetic field, the discontinuous change in positions of Bragg peaks disappears from the powder patterns (figure 5b). Rietveld refinement indicates that the system still undergoes the same cubic-to-tetragonal distortion beginning at a higher temperature ($T_C \cong 155$ K), which is consistent with the magnetic field- and temperature-dependent heat capacity data [27]. As seen in figure 5d, applied magnetic field completely eliminates phase volume discontinuity and the ferrimagnetic ordering becomes second order transformation.

Concluding remarks

Although not directly quoted in the two examples described above, the accuracy of the resultant structural information is exceptionally high, with the resolution of atomic positions being on the order of 10^{-2} Å [e.g., see 16]. This precision is standard in temperature dependent x-ray diffraction, yet in the past, it has not been realized in the presence of a strong magnetic field. Because of this excellent precision, magnetic field induced structural changes can now be directly imaged at the atomic resolution allowing for detailed structural analysis and further insight into the mechanisms that are responsible for these changes. In Gd_5Ge_4, the structural transformation occurs only if magnetic field exceeds 1 T, and it remains first order magnetostructural transition regardless of the magnetic field value between 1 and 4 T. In $DyCo_2$, magnetic field changes the nature of the phase transformation from the first order (zero and low field values) to the second order in a 4 T magnetic field.

References

1. Brister, K., 1997, *Rev. Sci. Instrum.* **68**, 1629.
2. Peterson, R.C. & Yang, H., 2001, *Rev. Mineral. Geochem.* **41**, 425.
3. Jenkins, R & Snyder, R.L., 1996, *Introduction to X-ray Powder Diffractometry* (New York: Wiley).
4. *Structure Determination from Powder Diffraction Data*, 2002, edited by W.I.F. David, K. Shankland, L.B. McCusker & Ch. Baerlocher (Oxford: Oxford University Press).
5. Pecharsky, V.K. & Zavalij, P.Y., 2003, *Fundamentals of Powder Diffraction and Structural Characterization of Materials* (New York: Kluwer Academic Publishers).
6. Nørgaard K., Eskildsen, M.R., Andersen, N.H., Jensen, J., Hedegard, P., Klausen, S. N. & Canfield, P.C., 2000, *Phys. Rev. Lett*. **84** 4982.
7. Pirogov, A., Podlesnyak, A., Strässle, T., Mirmelstein, A., Teplykh, A., Morozov, D., & Yermakov A., 2002, *Appl. Phys. A* **74**, S598.

8. Mira, J., Rivadula, F., Rivas, J., Fondado, A., Guidi, T., Caciuffo, R., Carsughi, F., Radaeli, P.G., Goodenough, J.B., 2003, *Phys. Rev. Lett*. **90**, 097203.
9. Young, R. A., 1993, *The Rietveld Method* (Oxford: Oxford University Press).
10. Ohsumi, H. & Tajima, K., 1998, *J. Phys. Soc. Japan* **67**, 1883.
11. Shimomura, S., Tajima, K., Wakabayashi, N., Kobayashi, S., Kuwahara, H. & Tokura, Y., 1999, *J. Phys. Soc. Japan* **68**, 1943.
12. Ma, Y., Awaji, S., Watanabe, K., Matsumoto, M. & Kobayashi, N., 2000, *Solid State Commun*. **113**, 671.
13. Gagliardi, M.S., Ren, Y., Mitchell, J.F. & Beno, M.A., 2004, *Appl. Phys. Lett*. **84**, 4538.
14. Watanabe, K., Watanabe, Y., Awaji, S., Fujiwara, M., Kobayashi, N. & Hasebe, T., 1998, *Adv. Cryogen. Engin*. **44B**, 747.
15. Pecharsky, V.K., Holm, A.P., Gschneidner, K.A., Jr. & Rink, R., 2003, *Phys. Rev. Lett*. **91**, 197204.
16. Holm, A.P., Pecharsky, V.K., Gschneidner, K.A., Jr., Rink, R. & Jirmanus, M.N., 2004, *Rev. Sci. Instrum*. **75**, 1081.
17. Pecharsky, V.K. & Gschneidner, K.A., Jr., 2007, *Pure Appl. Chem.* **79**, to be published (and references therein).
18. Pecharsky, V.K. & Gschneidner, K.A., Jr., 1997, Phys. Rev. Lett. **78**, 4494.
19. Levin, E.M., Pecharsky, V.K. & Gschneidner, K.A., Jr., 2001, *Phys. Rev. B* **63**, 174110.
20. Magen, C, Morellon, L., Algarabel, P.A., Marquina, C. & Ibarra M.R., 2003, *J. Phys.: Condens. Matter* **15**, 2389.
21. Roy, S.B., Chattopadhyay, M.K., Chaddah, P., Moore, J.D., Perkins, G.K., Cohen, L.F., Gschneidner, K.A., Jr. & Pecharsky, V.K., 2006, *Phys. Rev. B* **74**, 012403.
22. Mudryk, Ya., Holm, A.P., Gschneidner, K.A., Jr. & Pecharsky, V.K., 2005, *Phys. Rev. B* **72**, 064442.
23. Smith, G.S., Johnson, Q. & Tharp, A.G., 1967, *Acta Cryst*. **22**, 269.
24. Pecharsky, V.K. & Gschneidner, K.A., Jr., 1997, *J. Alloys Compds*. **260**, 98.
25. Duc, N.H. & Goto, T. *Handbook on the Physics and Chemistry of Rare Earths*, 1999, edited by K.A. Gschneidner, Jr. & L.R. Eyring (Amsterdam: Elsevier Science), vol. 26, 171.
26. Gratz, E.E., Bauer, E., Hausen, R., Maikis, M., Haen, P. & Markosyan, A.S., 1993, *Int. J. Mod. Phys.* **7**, 366.
27. Mudryk, Ya., Gschneidner, K.A., Jr. & Pecharsky, V.K. Unpublished.

Acknowledgements. This research was supported by the Division of Materials Science of the Office of Basic Energy Sciences of the US DOE under contract No. DE-AC02-07CH11358 with Iowa State University.